Ultra-fast hybrid method for predicting chemical shifts of ^{13}C: hybrid strategy with dynamic internal patterns and linear parameters

Atila Wuingryfi Reis Uchôa[1]

[1]Universidade Estadual do Maranhão (UEMA)

{Reis Uchôa, Atila Wuingryfi} atilauchoaoficial@hotmail.com

Abstract. *NMR spectroscopy is an essential tool for molecular characterization and structure elucidation, but the accurate prediction of chemical shifts in complex systems is still a challenge. In this study, we developed an ultrafast predictive model for ^{13}C chemical shifts, applied to a phenylpiperazine derivative, combining linear scaling and three direct internal standards: tetramethylsilane (TMS), methanol and benzene, using the HF/3-21G/DFT-MPW1PW91/6-31G(d) method. The proposed computational model, using methanol as the internal standard, reduced the average errors by more than 50%, outperforming computationally intensive methods described in the literature.*

Keywords: Chemical shifts; NMR spectroscopy; Predictive model.

Resumo. *A espectroscopia de RMN é uma ferramenta essencial para caracterização molecular e elucidação de estruturas, porém a predição precisa de deslocamentos químicos em sistemas complexos ainda representa um desafio. Neste estudo, desenvolvemos um modelo preditivo ultrarrápido para deslocamentos químicos de ^{13}C, aplicado a um derivado de fenilpiperazina, combinando escalonamento linear e três padrões internos diretos: tetrametilsilano (TMS), metanol e benzeno, utilizando o método HF/3-21G/DFT-MPW1PW91/6-31G(d). O modelo computacional, proposto, utilizando metanol como padrão interno, reduziu os erros médios em mais de 50%, superando métodos computacionalmente intensivos descritos na literatura.*

Palavras-chave: Deslocamentos químicos; Espectroscopia de RMN; Modelo preditivo.

1. Introduction

Nuclear Magnetic Resonance (NMR) spectroscopy has established itself as one of the most versatile and indispensable analytical techniques in the fields of chemistry and biochemistry. Its application ranges from the identification and characterization of complex organic molecules to the elucidation of chemical structures. However, the accurate assignment of NMR signals, especially in high molecular mass compounds, remains a significant challenge, requiring sophisticated analytical approaches (Gasevic et al., 2024; Kovács et al., 2023; Wang et al., 2021). In this scenario, quantum chemical simulations have emerged as essential tools, allowing spectra to be predicted and

helping to interpret experimental data with theoretical robustness (Borges et al., 2021; Yesiltepe et al., 2022).

To overcome the practical limitations of NMR, quantum simulations are predominantly based on density functional theory (DFT). In view of this, DFT stands out as a consolidated methodology, balancing performance and operational cost. Its effectiveness in predicting NMR chemical shifts has been widely validated in the literature, contributing to notable advances in accuracy and applicability, particularly in modeling ^{1}H and ^{13}C shifts (Cohen et al., 2023; Hansen et al., 2023; Pierens, 2014; Samultsev, Semenov and Krivdin, 2017; Venianakis, Siskos and Gerothanassis, 2024).

In the context of DFT, the calculation of isotropic shielding tensors for determining chemical shifts can be carried out by two main approaches. The first involves the use of a reference compound, such as tetramethylsilane (TMS), whose shielding tensor is calculated by the same method applied to the compound of interest, allowing a conversion factor to be obtained. The second approach, which is more widely accepted, is based on linear regression. In this method, multiple reference compounds are analyzed, correlating calculated shielding tensors with experimental chemical shifts to generate linear fitting protocols (Iron, 2017; Pierens, 2014; Semenov and Krivdin, 2019).

Computational linear fitting protocols based on DFT have proven effective in recent studies for different classes of compounds, as evidenced by work that has used different functionals and basis functions for specific systems. For example, Cardoso et al. (2021) used the mPW1PW91/6-31G(d) functional to elucidate savinin, while Alves et al. (2021) applied the B3LYP-6-311+G(d,p)/PBE0/aug-cc-pVDZ scheme to sesquiterpenes. Additionally, Costa et al. (2024) obtained accuracy in the prediction of ^{13}C shifts of loliolide with the GIAO-HSEh1PBE/6-31G* method, and Rocha et al. (2020) validated the GIAO-mPW1PW91/3-21G protocol for pentacyclic triterpenes.

However, the combination of hybrid methods (HF/DFT) with multiple internal standards for chemical shift calculations is still little explored, especially in phenylpiperazine derivatives, a class of pharmacological relevance (EL-Halaby et al., 2025). In this context, this study proposes to develop a robust predictive chemical shift model, using 22 structurally diverse molecules and three internal standards (TMS, methanol and benzene) for internal validation, using the combined HF-3-21G/DFT/MPW1PW91-6-31G(d) method. External validation was carried out with a phenylpiperazine derivative in order to assess the transferability of the predictive model to biologically relevant systems.

2. Methodology

To build the predictive model, 22 molecules from the internal training set were modeled three-dimensionally in the Avogadro software (Hanwell et al., 2012). The selection of these molecules was based on their prior testing and validation in the literature for molecular systems, demonstrating their effectiveness in building predictive models for chemical shifts. Furthermore, these molecules encompass a wide variety of functional groups, contributing to the robustness and generalizability of the model (Aliev, Courtier-Murias, and Zhou, 2009; Hanwell et al., 2012).

The molecular structures were initially geometrically pre-optimized using the GFN2-xTB method, implemented in the XTB (Extended Tight-Binding) computational

package (Bannwarth, Ehlert, and Grimme, 2019). Conformational analysis was then carried out using the CREST (Conformer-Rotamer Ensemble Sampling Tool) code (Pracht et al., 2020) with the GFN2-xTB method to identify and characterize the lowest-energy conformer. This conformational search was restricted to the target molecule from the external test set, as the molecules in the training set are structurally rigid. Subsequently, the lowest-energy conformers of both the target molecule and the training set structures were subjected to optimization calculations in Gaussian 09 (Frisch et al., 2009) using the Hartree-Fock (HF) method with the 3-21G basis set. The isotropic shielding tensors (σx) were determined using the GIAO (Gauge-Independent Atomic Orbital) method in conjunction with density functional theory (DFT). For these calculations, the MPW1PW91 hybrid functional combined with the 6-31G(d) basis function was used, a widely validated method for predicting chemical shifts (Sarotti, 2013; Zanardi and Sarotti, 2015). The theoretical chemical shifts of ^{13}C δ(cal) were obtained using Equation 1:

$$\delta_{cal} = \sigma_{ref} - \sigma x + \delta_{ref} \qquad (1)$$

Where σref represents the isotropic magnetic shielding of the reference standard, σx is the calculated isotropic magnetic shielding of the target compound and δref denotes the experimental chemical shift of the internal standard. Three calibration protocols were used: tetramethylsilane (TMS) (δref=0.00 ppm), methanol (δref=50.41 ppm) and benzene (δref=128.37 ppm) as an absolute reference, as established in the literature (Zanardi and Sarotti, 2015).

To develop the predictive model, a linear regression fit was made between the theoretical chemical deviations δ(cal) and the experimental chemical deviations (δ(exp). From this fit, the scale (a) and intercept (b) parameters were determined, as described in Equation 2:

$$y = ax + b \qquad (2)$$

To assess the generality of the method, the scale-up protocol was externally validated by applying it to the phenylpiperazine derivative 1-(naphthalen-1-yloxy)-3-(4-phenylpiperazin-1-yl)propan-2-ol (Figure 1). This compound was chosen because it has a complex molecular architecture, with heteroatoms, carbons in different states of hybridization and a variety of functional groups, characteristics that make it an ideal candidate for testing the robustness of the method.

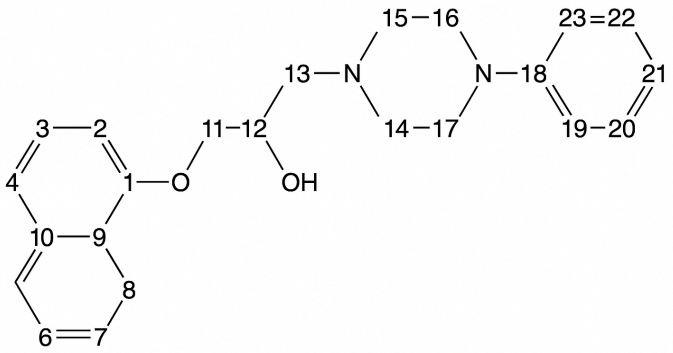

Figure 1 - Structure and molecular formula of the phenylpiperazine derivative.

The accuracy of the predictive models was statistically quantified using two

performance metrics: the Mean Absolute Deviation (MAD, Equation 3) and the Root Mean Square Deviation (RMSD, Equation 4).

$$MAD = \frac{1}{n}\sum_{i=n}^{n} = |x_i - \bar{x}| \qquad 3$$

$$RMSD = \sqrt{\frac{1}{n}\sum_{i=n}^{n} = |x_i - \bar{x}|^2} \qquad 4$$

2. Results and Discussion

Table 1 shows a detailed analysis of the spectroscopic data of the 22 compounds that make up the internal validation set. For each compound, the calculated chemical shifts δ(cal), the fitted chemical shifts δ(scal), values in relation to the three internal standards and the respective experimental δ(exp) values reported by Aliev, Courtier-Murias and Zhou (2009) and Zhang et al. (2007) are given, in addition to the MAD and RMSD statistical metrics calculated for each reference standard.

Table 1 - ^{13}C spectroscopic parameters spectroscopic parameters and statistical analysis for the set of 22 molecules.

	TMS	METHANOL	BENZENE	
Compounds	**δcal δ(scal)**	**δcal δ(scal)**	**δcal δ(scal)**	**δexp**
CH_4	-3,50 (-2,03)	-3,55 (-2,08)	-4,00 (-2,05)	-7,00
CH_3OH	50,45 (53,23)	50,41 (53,18)	57,96 (53,00)	51,50
C_2H_2	63,62 (66,70)	63,57 (66,65)	71,12 (66,42)	70,90
C_2H_4	116,45 (120,81)	116,4 (120,76)	123,96 (120,31)	123,60
C_2H_6	4,85 (6,53)	4,80 (6,48)	12,36 (6,48)	7,20
$H_2C{=}C{=}CH_2$	201,23 (207,62)	201,18 (207,57)	208,74 (206,79)	217,00
$H_2C{=}C{=}CH_2$	69,75 (72,79)	69,70 (72,94)	77,25 (72,67)	72,90
CH_2-CH_3-CH_2	14,78 (16,70)	14,73 (16,55)	22,29 (16,61)	15,60
CH_2-CH_3-CH_2	13,17 (15,05)	13,12 (15,00)	20,68 (14,96)	14,00
C_6H_6	120,86 (125,32)	120,81 (125,57)	129,37 (124,81)	130,90
CH_3F	68,90 (72,12)	68,85 (72,07)	76,41 (71,81)	71,30
CHF_3	120,48 (124,94)	120,43 (124,89)	128,00 (124,43)	119,70
CF_4	123,71 (128,25)	123,76 (128,20)	131,22 (127,72)	123,60
CO_2	115,78	115,73	123,29	129,90

	(120,12)	(120,07)	(119,63)	
CO	181,75 (187,68)	181,70 (187,63)	189,76 (186,92)	187,10
H_2CO	187,81 194,78	187,76 194,73	195,32 202,28	189,10
CH_3-CO-CH_3	194,78 (201,01)	194,73 (200,97)	202,28 (200,20)	201,20
CH_3-CO-CH_3	28,51 (30,76)	28,46 (30,71)	36,01 (30,71)	30,10
HCN	96,15 (100,02)	96,10 (99,97)	103,66 (99,61)	106,00
CH_2CN	1,35 (2,94)	1,30 (2,89)	8,85 (2,91)	0,40
CH_2CN	102,98 (107,01)	102,93 (106,96)	110,48 (106,57)	114,30
CH_3NH_2	29,35 (31,62)	29,30 (31,57)	36,86 (31,47)	29,80
CH_3CHO	26,26 (28,45)	26,21 (28,40)	33,77 (28,32)	30,90
CH_3CHO	192,39 (198,56)	192,33 (198,51)	199,98 (197,76)	194,80
OCS	151,11 (156,30)	151,06 (156,26)	158,82 (155,67)	158,10
CS_2	203,00 (209,44)	202,95 (209,39)	210,51 (208,59)	196,10
H_2CN_2	24,17 (26,32)	24,12 (26,27)	31,68 (26,19)	23,60
MAD	4,74 (3,70)	4,77 (3,69)	5,46 (3,71)	
RMSD	6,42 (4,91)	6,45 (4,92)	6,37 (4,94)	

The data (Table 1) show that the HF/3-21G/DFT/MPW1PW91-6-31G(d) method had a remarkable ability to predict chemical shifts, with results close to the experimental values. When using TMS as an internal standard, its performance was comparable to that of methanol, with a minimum difference of 0.03 ppm in the MAD. In relation to benzene, TMS showed a more significant advantage of 0.72 ppm in MAD. As for the RMSD, the variations were equally competitive: 0.03 ppm compared to methanol and 0.05 ppm compared to benzene. In this context, the protocol showed competitive results and, in some respects, was superior to the consolidated methods in the literature for the same set of molecules. For example, the MAD value obtained in this study, considering TMS = 4.74 ppm and methanol = 4.77 ppm, was lower than that reported by Aliev, Courtier-Murias and Zhou (2009), who used the B3LYP/6-311+G(2d,p) method and obtained 4.80 ppm. Similarly, the RMSD values, ranging from 4.91 to 6.45 ppm, were lower than those found by Costa et al. (2010) with the B3LYP/cc-pVXZ models, which showed a range of 5.89 to 11.10 ppm.

Figure 2 shows the linear correlation graph between the theoretical and experimental chemical shifts of the 22 molecules in the internal validation set, considering different internal standards (TMS, methanol and benzene). In this context,

although the calculated chemical shift values (δ_{cal}) proved to be acceptable for the set of 22 molecules, the application of the predictive model for internal validation (Figure 2) resulted in significant improvements: with TMS, a 22% reduction was observed in the MAD (3.70 ppm) and 24% in the RMSD (4.91 ppm); for methanol, there was a 23% reduction in both metrics (MAD=3.69 and RMSD=4.91 ppm) and, for benzene, the reductions were 32% in the MAD (3.71 ppm) and 22% in the RMSD (4.94 ppm).

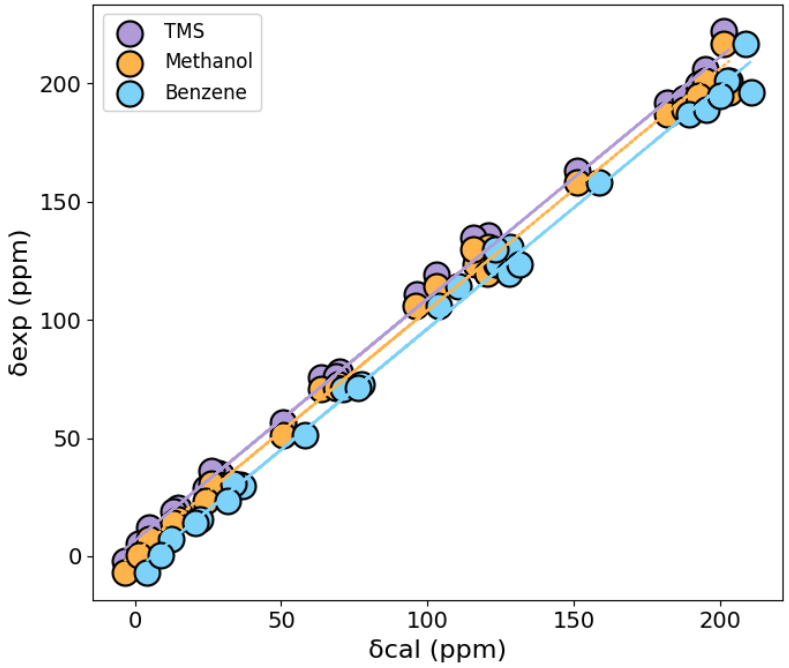

Figure 2 - Correlation between the experimental and theoretical ^{13}C chemical hifts of the internal test set.

It is noteworthy that the predictive model scaled from the hybrid HF/3-21G/DFT/MPW1PW91/6-31G(d) method, using the benzene internal standard, showed an efficiency comparable to that of more computationally intensive protocols for the same set of molecules, such as the B3LYP/6-311+G(2d,p)/HF/6-31G(d) reported by Zhang et al. (2007), which showed a MAD of 2.72 ppm, and OPBE/6-311+G(2d,p) by Kingston (1991), with a MAD of 2.85 ppm and an RMSD of 4.46 ppm.

Equations 5, 6 and 7 make up the core of the predictive model, expressed in the form y = ax + b, and were used to calculate the scaled chemical displacements δ(scal) from the calculated values δ(cal). The Pearson correlation coefficient obtained for all the models was 0.098

$$\delta_{scal} = 1{,}02.\ \delta_{cal(TMS)}\mathrm{HF/321G/MPW91PW91/631G(d)} - 1{,}56 \qquad (5)$$

$$\delta_{scal} = 1{,}02.\ \delta_{cal(METHANOL)}\mathrm{HF/321G/MPW91PW91/631G(d)} + 1{,}61 \qquad (6)$$

$$\delta_{scal} = 1{,}02.\ \delta_{cal(BENZENE)}\mathrm{HF/321G/MPW91PW91/631G(d)} - 6{,}13 \qquad (7)$$

Analysis of the absolute errors (Figure 3) shows that, for TMS and methanol, the greatest deviations occur in compounds containing sp carbons, such as $H_2C=C=CH_2$ (15.76 ppm for TMS; 15.81 ppm for methanol) and CO_2 (14.11 ppm for TMS; 14.16 ppm for methanol), while the smallest errors are observed for sp^3 carbons, such as CF_4 (0.11 ppm for TMS; 0.06 ppm for methanol) and CH_3NH_2 (0.44 ppm for TMS; 0.49 ppm for methanol). In the case of benzene, the largest errors emerged in CS_2 (14.41 ppm) and CH_4 (11.00 ppm), whereas the smallest deviations were recorded in C_2H_2 (0.22 ppm) and OCS (0.52 ppm).

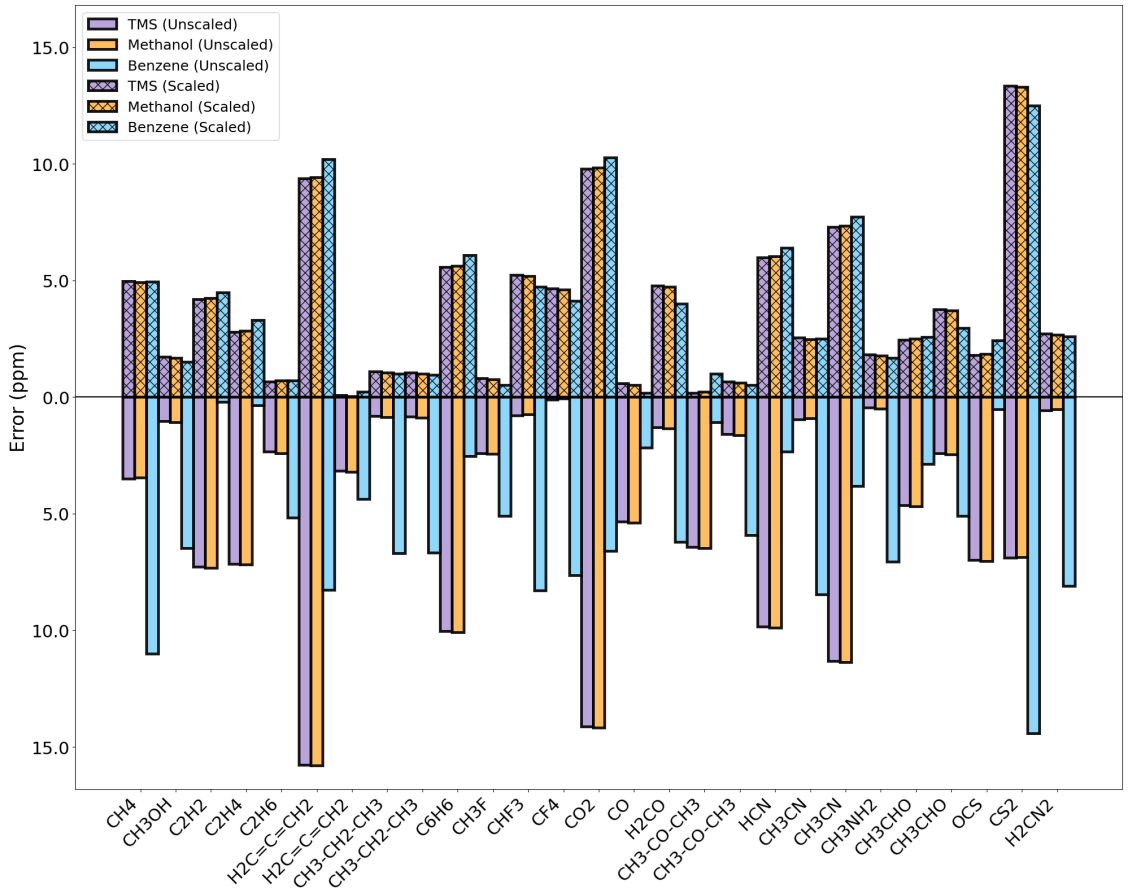

Figure 3 - Error graph between the experimental and theoretical chemical shifts of ^{13}C for the internal test set.

However, linear scaling significantly reduced the absolute errors, with corrections of more than 90% in the sp2 carbon of the compounds CH_3-CO-CH_3 and C_2H_6 standing out. For TMS, the sp2 carbon of CH_3-CO-CH_3 had its error reduced from 15.76 ppm to 9.37 ppm, and CO_2 from 14.11 ppm to 9.77 ppm. In methanol, the error in carbon sp $H_2C=C=CH_2$ went from 15.81 ppm to 9.42 ppm, and CO_2 from 14.16 ppm to 9.82 ppm. For the internal standard, Benzene, CH_4 had its error reduced from 11.00 ppm to 4.95 ppm, and CS_2 from 14.41 ppm to 12.49 ppm. These reductions highlight the effectiveness of scaling in correcting errors in chemical shifts, regardless of the internal standard used.

Conformational analysis of the phenylpiperazine derivative revealed that structures 1 and 2 are the most stable, with a population of 12.5% each at equilibrium (see Table 2). Subsequent conformations (3 to 20) showed gradual increases in energy,

ranging from 0.46 to 1.57 kcal mol-¹, accompanied by progressive reductions in population, ranging from 0.057% to 0.009%. Conformations with minimal energy differences, such as 14 and 15, had practically identical populations (0.016%). Conformation 20, with an energy of 1.57 kcal mol-¹ and a population of 0.009%, represented the least favored state, being 1.6 kcal mol-¹ above the lowest energy conformation.

Table 2 - Conformers, energies and the respective Boltmzann populations of the phenylpiperazine derivative.

Conformation	Energy (kcal mol^{-1})	Population Boltzmann (%)
1	0,00	12,5
2	0,00	12,5
3	0,46	5,7
4	0,50	5,4
5	0,62	4,4
6	0,71	3,7
7	0,62	4,3
8	0,65	4,2
9	0,70	3,8
10	0,74	3,6
11	0,89	2,8
12	0,95	2,5
13	0,96	2,5
14	1,23	1,6
15	1,23	1,6
16	1,30	1,4
17	1,36	1,2
18	1,48	1,0
19	1,52	1,0
20	1,57	0,9

Table 3 shows the comparative analysis between the calculated chemical shifts δ(cal), scaled δ(scal) (using the predictive models shown in Figure 2) for the phenylpiperazine derivative and the experimental values (δexp) reported by Xiao et al. (2005). Here, σref corresponds to the isotropic magnetic shielding of the reference standard, σ is the isotropic shielding of the target compound and δref denotes the experimental chemical shift of the internal standard. The results showed that the hybrid HF/3-21G/DFT/MPW1PW91/6-31G(d) method employed provided predictions with reasonable agreement with the experimental values. Among the internal references, benzene stood out as having the best performance, with differences of 1.85 ppm compared to TMS and 1.58 ppm compared to methanol. Furthermore, when analyzing the RMSD (Mean Square Deviation), the variations were 0.94 ppm for TMS and 0.64 ppm for methanol, reinforcing the greater precision obtained when using benzene as a direct reference. Although the chemical shift values calculated for the phenylpiperazine derivative were acceptable, the application of the linear scale was fundamental in significantly improving the accuracy of the results, regardless of the internal standard

used.

Table 3 - ^{13}C spectroscopic parameters and statistical analysis for the phenylpiperazine derivative.

	TMS	Methanol	Benzene	
	δcal δscal	δcal δscal	δcal δscal	δexp
C1	145,84 (150,31)	146,25 (150,79)	153,81 (150,75)	154,34
C2	97,35 (100,86)	97,76 (101,33)	105,32 (101,29)	104,85
C3	118,92 (122,84)	119,32 (123,31)	126,88 (123,28)	125,79
C4	114,23 (118,07)	114,64 (118,54)	122,20 (118,51)	120,60
C5	120,35 (124,32)	120,77 (124,79)	128,32 (124,76)	127,49
C6	119,36 (123,31)	119,78 (123,78)	127,33 (123,75)	126,43
C7	118,11 (122,03)	118,52 (122,50)	126,08 (122,47)	125,24
C8	118,46 (122,39)	118,88 (122,86)	126,43 (122,83)	121,86
C9	117,68 (121,59)	118,09 (122,06)	125,65 (122,03)	125,54
C10	126,76 (130,86)	127,17 (131,33)	134,73 (131,29)	134,46
C11	70,09 (73,05)	70,50 (73,52)	78,06 (73,49)	70,43
C12	65,64 (68,51)	66,05 (68,98)	73,60 (68,95)	65,67
C13	63,03 (64,83)	62,44 (65,30)	70,00 (65,27)	60,87
C14	49,93 (52,49)	50,34 (52,96)	57,90 (52,92)	53,37
C15	47,24 (49,74)	47,65 (50,21)	55,20 (50,18)	53,37
C16	53,73 (56,37)	54,15 (56,84)	61,70 (56,81)	49,25
C17	48,00 (50,52)	48,41 (50,99)	55,97 (50,95)	49,26
C18	145,06 (149,52)	145,47 (149,99)	153,02 (149,95)	151,13
C19	116,41 (120,30)	116,82 (120,77)	124,38 (120,74)	116,12
C20	121,24 (125,22)	121,65 (125,69)	129,21 (125,66)	129,13
C21	113,87 (117,71)	114,29 (118,18)	121,84 (118,15)	119,88
C22	121,38 (125,37)	121,79 (125,84)	129,35 (125,80)	129,13

C23	111,25 (115,03)	111,66 (115,50)	119,21 (115,47)	116,12
MAD	5,19 (2,60)	4,92 (2,01)	3,34 (2,45)	
RSMD	5,42 (3,09)	5,12 (2,56)	4,48 (2,99)	

The application of linear correction using TMS as the internal reference resulted in a reduction of 49.9% in the mean absolute deviation (MAD = 2.60 ppm) and 43.0% in the root mean square deviation (RMSD = 3.09 ppm). Methanol, however, proved to be an even more effective internal standard, reducing the MAD by 59.2% (to 2.01 ppm) and the RMSD by 50.0% (to 2.56 ppm), thereby enhancing the accuracy of the predictive protocol. In contrast, benzene yielded more modest improvements, with reductions of 26.0% (MAD = 2.45 ppm) and 33.3% (RMSD = 2.99 ppm).

When compared to existing models in the literature, the predictive protocol based on HF/3-21G/DFT/MPW1PW91/6-31G(d) demonstrated superior performance. For instance, it outperformed the HF/6-31G(d)/STO-3G method employed by Cheeseman et al. (1996), which, when applied to external molecules, yielded higher MAD and RMSD values (4.96 ppm and 6.43 ppm, respectively). Additionally, the proposed approach surpassed the hybrid B3LYP/6-311+G(2d,p) scheme reported by Aliev, Courtier-Murias, and Zhou (2009), which exhibited inferior external validation results, with MAD ranging from 2.90 to 6.45 ppm and RMSD from 3.10 to 7.44 ppm.

Analysis of the absolute errors of the chemical shifts of the phenylpiperazine derivative, shown in Figure 4, reveals that for TMS, the greatest deviations are associated with carbon C1 (8.50 ppm), with a reduction of 52.6% (to 4.03 ppm), followed by C20 (7.89 ppm) with a reduction of 50.5% (to 3.90 ppm), and C7 (7.86 ppm) with a reduction of 49.9% (to 3.94 ppm).

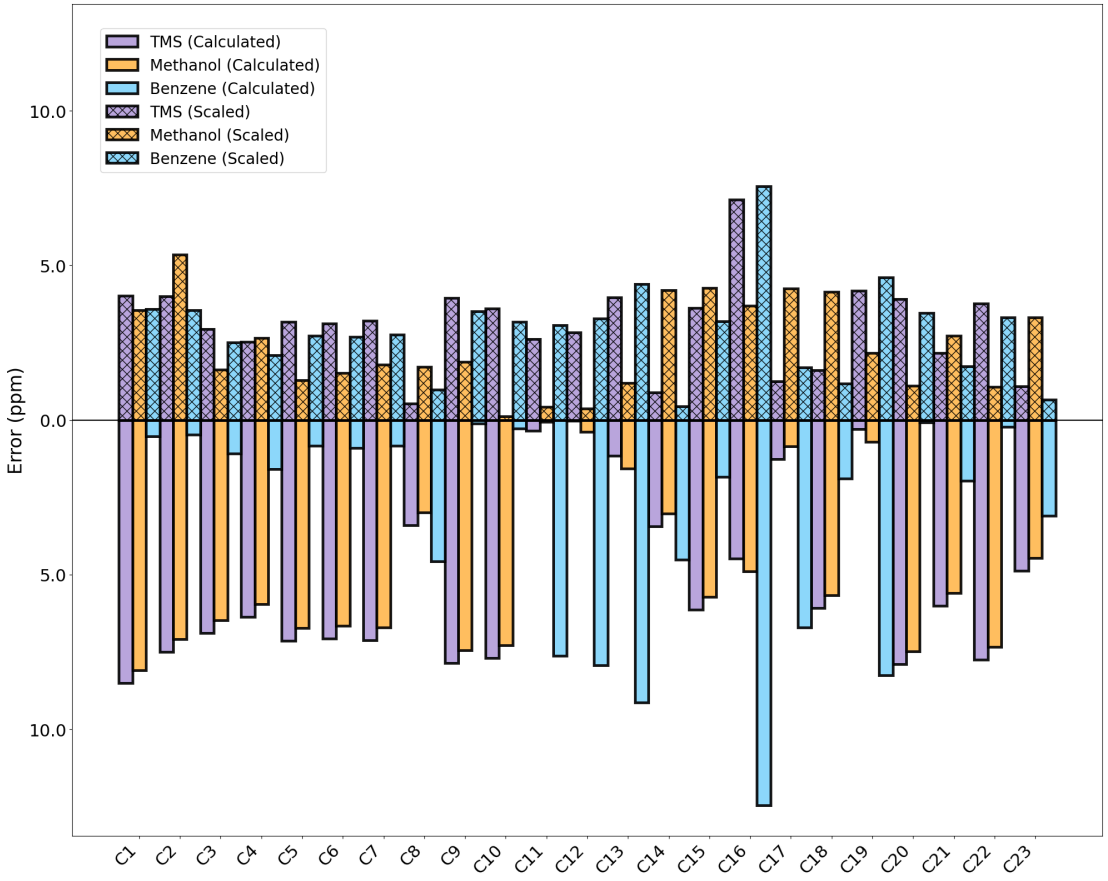

Figure 4 - Error graph between the experimental and theoretical chemical shifts of ^{13}C for the phenylpiperazine derivative.

For methanol, carbon C1 (8.09 ppm) also showed a notable reduction of 56.0% (to 3.56 ppm), followed by C6 (6.65 ppm) with a reduction of 77.3% (to 1.51 ppm) and C7 (6.72 ppm) with a reduction of 73.4% (to 1.79 ppm). In the case of benzene, significant reductions were recorded for C8 (4.57 ppm), with a reduction of 78.8% (to 0.97 ppm), and C18 (1.89 ppm), with a reduction of 37.6% (to 1.18 ppm), highlighting the effectiveness of the linear adjustment regardless of the internal standard used for the phenylpiperazine derivative.

4 Conclusion

This study established an ultrafast hybrid computational protocol for predicting ^{13}C chemical shifts, validated with 22 organic compounds and three internal standards. After linear scaling, the calculated chemical shifts for the internal set showed error reductions of up to 32% in the mean absolute deviation (MAD) using benzene and 24% in the root mean square deviation (RMSD) with TMS, underscoring the model's efficiency across different internal references. In the external validation, predictive models derived from the internal set successfully reproduced the ^{13}C chemical shifts of a phenylpiperazine derivative with high accuracy, reducing MAD by up to 59.2% (MAD = 2.01 ppm) and RMSD by 50% (RMSD = 2.56 ppm). Among the internal standards, methanol stood out

as the most effective, confirming the model's applicability to the phenylpiperazine derivative and suggesting its potential extension to more complex molecules with similar structural features, such as condensed or fused ring systems containing conjugated π orbitals, heteroatoms, and diverse functional groups.

The efficiency of the predictive models, both in internal calibration and external validation, generated by the hybrid HF/3-21G/DFT/MPW1PW91/6-31G(d) method, positions this protocol as a competitive and, in some respects, superior alternative to classical computational approaches reported in the literature for ^{13}C NMR simulations, in terms of accuracy and computational efficiency. In summary, the proposed ultrafast computational protocol offers a promising tool for ^{13}C chemical shift prediction, facilitating the structural elucidation and virtual screening of bioactive and structurally complex compounds.

Bibliographical References

Aliev, A. E., Courtier-Murias, D., & Zhou, S. (2009). Scaling factors for carbon NMR chemical shifts obtained from DFT B3LYP calculations. *Journal of Molecular Structure: Theochem*, 893(1–3), 1–5.

Alves, G. S., Cardoso, E. F., Souza, S. S., Albuquerque, A. C. F., Martins, R. C. C., Miranda, R. S., Silva, F. B., Siqueira, M. R. S., Santos Junior, F. M., & Mota, G. V. S. (2021). 13C NMR calculations through GIAO, CSGT, and IGAIM approaches: Scaling factors for terpenes. *Brazilian Journal of Development*, 7(3), 21247–21257.

Bannwarth, C., Ehlert, S., & Grimme, S. (2019). GFN2-xTB—An accurate and broadly parametrized self-consistent tight-binding quantum chemical method with multipole electrostatics and density-dependent dispersion contributions. *Journal of Chemical Theory and Computation,* 15(3), 1652–1671.

Borges, R. M., Colby, S. M., Das, S., Edison, A. S., Fiehn, O., Kind, T., Lee, J., Merrill, A. T., Merz, K. M., & Metz, T. O. (2021). Quantum chemistry calculations for metabolomics. *Chemical Reviews*, 121(10), 5633–5670.

Cardoso, E. F., Alves, G. S., Souza, S. S., Albuquerque, A. C. F., Martins, R. C. C., Miranda, R. S., Silva, F. B., Siqueira, M. R. S., Santos Junior, F. M., & Mota, G. V. S. (2021). Combination of scaling factors of ^{13}C and 1H NMR chemical shifts (based on linear regressions) and neural networks to assist in structural determination of savinin. *Brazilian Journal of Development*, 7(3), 22930–22939.

Cheeseman, J. R., Trucks, G. W., Keith, T. A., & Frisch, M. J. (1996). A comparison of models for calculating nuclear magnetic resonance shielding tensors. *The Journal of Chemical Physics*, 104(14), 5497–5509.

Cohen, R. D., Wood, J. S., Lam, Y.-H., Buevich, A. V., Sherer, E. C., Reibarkh, M., Williamson, R. T., & Martin, G. E. (2023). DELTA50: A highly accurate database of experimental ^{1}H and ^{13}C NMR chemical shifts applied to DFT benchmarking. *Molecules*, 28(6), 2449.

Costa, F. L. P., Albuquerque, A. C. F., Santos, F. M., & Amorim, M. B. (2010). GIAO‐HDFT scaling factor for 13C NMR chemical shifts calculation. Journal of *Physical Organic Chemistry*, 23(10), 972–977.

Costa, F. L. P., Mota, G. V. S., Siqueira, M., & Chaves Neto, A. M. J. (2024). Scaling

factors of 13C NMR Δ: Comparison of different hybrid functionals and basis sets. *Journal Chemical Processes Magazine*, 18(35), 51–55.

El-Halaby, L. O., Al-Sanea, M. M., Elgazar, A. A., Tawfik, S. S., Hamdi, A., & Ewes, W. A. (2025). New phenylpiperazine-thiazolidine-2,4-dione hybrids targeting MAO inhibition: Synthesis, biological evaluation, kinetic study and in silico insights. *Bioorganic & Medicinal Chemistry*, 121, 118123.

Frish, J., Vreven, T., Kudin, K. N., Burant, J. C., Millam, J. M., Iyengar, S. S., Tomasi, J., Barone, V., Mennucci, B., Cossi, M., Scalmani, G., Rega, N., Petersson, G. A., Nakatsuji, H., ... & Pople, J. A. (2004). Gaussian 09, Revision C.01. Gaussian Inc.

Gasevic, T., Büning, J. B. K., Grimme, S., & Bursch, M. (2024). Benchmark study on the calculation of 207Pb NMR chemical shifts. *Inorganic Chemistry*, 63(11), 5052–5064.

Hanwell, M. D., Curtis, D. E., Lonie, D. C., Vandermeersch, T., Zurek, E., & Hutchison, G. R. (2012). Avogadro: An advanced semantic chemical editor, visualization, and analysis platform. *Journal of Cheminformatics*, 4(1), 17.

Hansen, P. E., Darugar, V., Vakili, M., & Kamounah, F. S. (2023). Tautomerism of pyridinylbutane‐1,3‐diones: An NMR and DFT study. *Magnetic Resonance in Chemistry*, 61(6), 356–362.

Iron, M. A. (2017). Evaluation of the factors impacting the accuracy of ^{13}C NMR chemical shift predictions using density functional theory—The advantage of long-range corrected functionals. *Journal of Chemical Theory and Computation*, 13(11), 5798–5819.

Kingston, D. G. I. (1991). The chemistry of taxol. *Pharmacology & Therapeutics*, 52(1), 1–34.

Kovács, T., Lajter, I., Kősz, N., Schelz, Z., Bózsity-Faragó, N., Borbás, A., Zupkó, I., Krupitza, G., Frisch, R., & Hohmann, J. (2023). Isolation and NMR scaling factors for the structure determination of Lobatolide H, a flexible sesquiterpene from Neurolaena lobata. *International Journal of Molecular Sciences*, 24(6), 5841.

Pierens, G. K. (2014). ^{1}H and ^{13}C NMR scaling factors for the calculation of chemical shifts in commonly used solvents using density functional theory. *Journal of Computational Chemistry*, 35(18), 1388–1394.

Pracht, P., Grimme, S., Bannwarth, C., Bohle, F., Ehlert, S., Feldmann, G., Gorges, J., Müller, M., Neudecker, T., Plett, C., Spicher, S., Steinbach, P., Wesołowski, P. A., & Zeller, F. (2024). CREST—A program for the exploration of low-energy molecular chemical space. *The Journal of Chemical Physics*, 160(11), 114110.

Rocha, R. A. M., Giacomello, T. F., Chaves Neto, A. M. J., Mota, G. V. S., & Costa, F. L. P. (2020). 1^{3}C NMR chemical shift calculation applied to differentiation of regioisomers triterpenes. *Virtual Journal of Chemistry*, 12(4), 913–929.

Samultsev, D. O., Semenov, V. A., & Krivdin, L. B. (2017). On the accuracy factors and computational cost of the GIAO–DFT calculation of ^{15}N NMR chemical shifts of amides. *Magnetic Resonance in Chemistry*, 55(11), 1015–1021.

Sarotti, A. M. (2013). Successful combination of computationally inexpensive GIAO ^{13}C NMR calculations and artificial neural network pattern recognition: A new

strategy for simple and rapid detection of structural misassignments. *Organic & Biomolecular Chemistry*, 11(29), 4847.

Semenov, V. A., & Krivdin, L. B. (2019). DFT computational schemes for ^{1}H and ^{13}C NMR chemical shifts of natural products, exemplified by strychnine. *Magnetic Resonance in Chemistry*, 58(1), 56–64.

Venianakis, T., Siskos, M. G., & Gerothanassis, I. P. (2024). DFT calculations of ^{1}H and ^{13}C NMR chemical shifts of hydroxy secondary oxidation products of geometric isomers of conjugated linoleic acid methyl esters: Structures in solution and revision of NMR assignments. *Magnetic Resonance in Chemistry*, 63(3), 227–240.

Wang, M., Sun, X., Luo, W., Božović, S., Gong, C., & Ren, J. (2021). Characterization and analysis of antioxidant activity of walnut-derived pentapeptide PW5 via nuclear magnetic resonance spectroscopy. *Food Chemistry*, 339, 128047.

Xiao, Z., Yuan, M., Zhang, S., Wu, J., Qi, S., & Li, Q. (2005). Complete assignments of 1H and ^{13}C NMR data for ten phenylpiperazine derivatives. *Magnetic Resonance in Chemistry*, 43(10), 869–872.

Yesiltepe, Y., Govind, N., Metz, T. O., Pan, C., Webb-Robertson, B.-J. M., Ulrich, E. L., ... & Smith, R. D. (2022). An initial investigation of accuracy required for the identification of small molecules in complex samples using quantum chemical calculated NMR chemical shifts. *Journal of Cheminformatics,* 14, 64.

Zanardi, M. M., & Sarotti, A. M. (2015). GIAO C–H COSY simulations merged with artificial neural networks pattern recognition analysis: Pushing the structural validation a step forward. *The Journal of Organic Chemistry,* 80(19), 9371–9378.

Zhang, Y., Wu, A., Xu, X., & Yan, Y. (2007). Geometric dependence of the B3LYP-predicted magnetic shieldings and chemical shifts. *The Journal of Physical Chemistry A,* 111(38), 9431–9437.